Microscopic particle-rotor model for low-lying spectrum of Λ hypernuclei

H. Mei[a,b], K. Hagino[a,c], J.M. Yao[a,b], T. Motoba[d,e]

[a]*Department of Physics, Tohoku University, Sendai 980-8578,Japan*
[b]*School of Physical Science and Technology, Southwest University, Chongqing 400715, China*
[c]*Research Center for Electron Photon Science, Tohoku University, 1-2-1 Mikamine, Sendai 982-0826, Japan*
[d]*Laboratory of Physics, Osaka Electro-Communications University, Neyagawa 572-8530, Japan*
[e]*Yukawa Institute for Theoretical Physics, Kyoto University, Kyoto 606-8502, Japan*

arXiv:1406.4604v1 [nucl-th] 18 Jun 2014

Abstract

We propose a novel method for low-lying states of hypernuclei based on the particle-rotor model, in which hypernuclear states are constructed by coupling the hyperon to low-lying states of the core nucleus. In contrast to the conventional particle-rotor model, we employ a microscopic approach for the core states, that is, the generator coordinate method (GCM) with the particle number and angular momentum projections. We apply this microscopic particle-rotor model to ${}^{9}_{\Lambda}$Be employing a point-coupling version of the relativistic mean-field Lagrangian. A reasonable agreement with the experimental data for the low-spin spectrum is achieved using the Λ*N* coupling strengths determined to reproduce the binding energy of the Λ particle.

Keywords:
Hypernuclei, Low-lying states, Covariant density functional theory, Beyond mean-field approximation

Introduction.– In the past decade, many high-resolution γ-ray spectroscopy experiments have been carried out for *p*-shell Λ-hypernuclei [1, 2]. The measured energy spectra and electric multipole transition strengths in the low-lying states provide rich information on the Λ-nucleon interaction in nuclear medium and on the impurity effect of Λ particle on nuclear structure. In this context, several interesting phenomena have been disclosed. One of the most important findings is the appreciable shrinkage of the nuclear core due to the Λ participation [3, 4, 5], for which a theoretical prediction has been clearly confirmed in the experiment [6].

The theoretical studies of γ-ray spectroscopy for *p*-shell hypernuclei have been mainly performed with the cluster model [3, 5, 7, 8] and with the shell model [9, 10, 11]. Recently, an ab-initio method as well as the antisymmetrized molecular dynamics (AMD) have also been extended in order to study low-lying states of hypernuclei [12, 13]. Most of these models, however, have been limited to light hypernuclei while it may be difficult to apply them to medium-heavy and heavy hypernuclei.

A self-consistent mean-field approach offers a way to study globally the structure of atomic nuclei as well as hypernuclei from light to heavy systems [14], although the pure mean-field approximation does not yield a spectrum of nuclei due to the broken symmetries. In the recent decade, the self-consistent mean-field models have been applied to study the impurity effect of Λ particle on the nuclear deformation of *p*- and *sd*-shell Λ hypernuclei [15, 16, 17, 18, 19, 20, 21]. It has been found that the shape polarization effect of Λ hyperon is in general not prominent, except for a few exceptions, including ${}^{13}_{\Lambda}$C, ${}^{23}_{\Lambda}$C, and ${}^{29,31}_{\Lambda}$Si [16].

These mean-field studies have shown that the potential energy surface of a hypernucleus is generally softer against deformation than that of the corresponding core nucleus. This implies that the shape fluctuation effect, which is not included in the pure mean-field approximation, will be more important in hypernuclei than in normal nuclei. Furthermore, in order to connect mean-field results to spectroscopic observables, such as $B(E2)$ values, one has to rely on additional assumptions such as the rigid rotor model, which however would not work for, *e.g.*, nuclei with small deformation or with shape coexistence. To quantify the impurity effect of Λ particle on nuclear structure, one thus has to go beyond the pure mean-field approximation.

Recently, we have quantitatively studied the impurity effect of Λ hyperon on the low-lying states of ^{24}Mg by using a five-dimensional collective Hamiltonian as a choice of the beyond mean-field approaches [22]. To this end, we have used parameters determined by triaxially deformed Skyrme-Hartree-Fock+BCS calculations. We have applied this method to transition strengths and found that the presence of one Λ hyperon in the $s_{1/2}$ orbital in ^{24}Mg reduces the $B(E2: 2^+_1 \rightarrow 0^+_1)$ by 9%. However, low-lying spectra of a whole single-Λ hypernucleus have been difficult to calculate due to the unpaired Λ particle.

In fact, a beyond mean-field calculation for low-lying states of odd-mass nuclei based on modern energy density functionals is a long-standing problem in nuclear physics. One important reason for the difficulty is that the last unpaired nucleon breaks some of the symmetries. Moreover, due to the pairing correlation, many quasi-particle configurations are close in energy and will be strongly mixed with each other. Both of these facts complicate a calculation for low-lying spectra of odd-mass nuclei at the beyond mean-field level, although some attempts have been made recently based on the Skyrme energy density functional [23].

In this paper, we propose a novel microscopic particle-rotor

model for the low-lying states of single-Λ hypernuclei. The novel feature is that we combine the motion of Λ particle with the core nucleus states, which are described by the state-of-the-art covariant density functional approach, that is, the generator coordinate method (GCM) based on the relativistic mean-field (RMF) approach supplemented with the particle number and the angular momentum projections.

The particle-rotor model was firstly proposed by Bohr and Mottelson [24] (see also Ref. [25]), and has recently been applied also to study the structure of odd-mass neutron-rich nuclei, such as ^{11}Be [26, 27], ^{15,17,19}C [28], and ^{31}Ne [29]. In this model, the motion of a valence particle is coupled to the rotational motion of a deformed core nucleus, which is usually described by the rigid rotor model. The Pauli principle between the valence nucleon and the nucleons in the core nucleus is treated approximately. In contrast to this conventional particle-rotor model, in this paper we construct low-lying states of the nuclear core microscopically. That is, we superpose many quadrupole deformed RMF+BCS states, after both the particle-number and the angular-momentum projections are carried out [30]. A similar idea as the microscopic particle-rotor model has recently been employed by Minomo *et al.* in order to describe the structure of the one-neutron halo nucleus ^{31}Ne with AMD [31]. We apply this microscopic particle-rotor model to hypernuclei, for which the Pauli principle between the valence Λ particle and the nucleons in the core nucleus is absent. We will demonstrate the applicability of this method by studying the low-lying spectrum of $^{9}_{\Lambda}$Be.

Formalism.– We describe a single-Λ hypernucleus as a system in which a Λ hyperon interacts with nucleons inside a nuclear core via a scalar and vector contact couplings. The Lagrangian for the single-Λ hypernucleus then reads,

$$\mathcal{L} = \mathcal{L}_{\rm free} + \mathcal{L}_{\rm em} + \mathcal{L}^{NN}_{\rm int} + \mathcal{L}^{N\Lambda}_{\rm int}, \tag{1}$$

where $\mathcal{L}_{\rm free}$ is the free part of the Lagrangian for the nucleons and the hyperon, $\mathcal{L}_{\rm em}$ is the standard electromagnetic Lagrangian, and $\mathcal{L}^{NN}_{\rm int}$ is the effective strong interaction between nucleons. We employ a similar form for the $N\Lambda$ effective interaction term $\mathcal{L}^{N\Lambda}_{\rm int}$ as in Ref. [32], and therefore, the vector and scalar $N\Lambda$ interaction terms $\hat{V}^{N\Lambda}_V$ and $\hat{V}^{N\Lambda}_S$ are given by

$$\hat{V}^{N\Lambda}_V(\boldsymbol{r}_\Lambda, \boldsymbol{r}_N) = \alpha^{N\Lambda}_V \delta(\boldsymbol{r}_\Lambda - \boldsymbol{r}_N) \tag{2}$$
$$\hat{V}^{N\Lambda}_S(\boldsymbol{r}_\Lambda, \boldsymbol{r}_N) = \alpha^{N\Lambda}_S \gamma^0_\Lambda \delta(\boldsymbol{r}_\Lambda - \boldsymbol{r}_N)\gamma^0_N, \tag{3}$$

respectively. For simplicity, the higher-order coupling terms and the derivative terms in the $N\Lambda$ interaction are not taken into account in the present study.

Based on the idea of particle-rotor model, we construct the wave function for single-Λ hypernuclei with an even-even nuclear core as

$$\Psi_{IM}(\boldsymbol{r}_\Lambda, \{\boldsymbol{r}_N\}) = \sum_{j\ell I_c} \mathscr{R}_{j\ell I_c}(r_\Lambda) \mathscr{F}^{IM}_{j\ell I_c}(\hat{\boldsymbol{r}}_\Lambda, \{\boldsymbol{r}_N\}), \tag{4}$$

where

$$\mathscr{F}^{IM}_{j\ell I_c}(\hat{\boldsymbol{r}}_\Lambda, \{\boldsymbol{r}_N\}) = [\mathscr{Y}_{j\ell}(\hat{\boldsymbol{r}}_\Lambda) \otimes \Phi_{I_c}(\{\boldsymbol{r}_N\})]^{(IM)} \tag{5}$$

with $\boldsymbol{r}_\Lambda$ and $\boldsymbol{r}_N$ being the coordinates of the Λ hyperon and the nucleons, respectively. In this equation, I is the total angular momentum and M is its projection onto the z-axis for the whole Λ hypernucleus. $\mathscr{R}_{j\ell I_c}(r_\Lambda)$ and $\mathscr{Y}_{j\ell}(\hat{\boldsymbol{r}}_\Lambda)$ are the four-component radial wave function and the spin-angular wave function for the Λ hyperon, respectively.

In the microscopic particle-rotor model, the wave function for the nuclear core part, $\Phi_{I_cM_c}(\{\boldsymbol{r}_N\})$, is given as a superposition of particle-number and angular-momentum projected RMF+BCS states, $|\varphi(\beta)\rangle$, that is,

$$|\Phi_{I_cM_c}\rangle = \sum_\beta f_{I_cNZ}(\beta) \hat{P}^{I_c}_{M_cK} \hat{P}^N \hat{P}^Z |\varphi(\beta)\rangle, \tag{6}$$

where $\hat{P}^{I_c}_{M_cK}$, $\hat{P}^N$, $\hat{P}^Z$ are the projection operators onto good numbers of angular momentum, neutrons and protons, respectively. The mean-field wave functions $|\varphi(\beta)\rangle$ are a set of Slater determinants of quasi-particle states with different quadrupole deformation β. For simplicity, we consider only the axial deformation for the nuclear core and thus the K quantum number is zero in Eq. (6). The weight factor $f_{I_cNZ}(\beta)$ is determined by solving the Hill-Wheeler-Griffin equation. We call this scheme a generator coordinate method (GCM) plus particle-number (PN) and one-dimensional angular-momentum (1DAM) projections, GCM+PN1DAMP. See Ref. [30] for more details on the GCM calculation for the nuclear core states.

Substituting Eq. (4) to the Dirac equation for the whole hypernucleus, $H|\Psi_{IM}\rangle = E_I|\Psi_{IM}\rangle$, where H is the relativistic Hamiltonian corresponding to Eq. (1), one can derive the coupled-channels equations for $\mathscr{R}_{j\ell I_c}(r_\Lambda)$, in which the coupling potentials are given in terms of the transition densities. From the solutions of those equations, one can compute the probability for the $(j\ell I_c)$ component in the total wave function, Ψ_{IM}, as

$$P_{j\ell I_c} = \int_0^\infty r^2_\Lambda dr_\Lambda \, |\mathscr{R}_{j\ell I_c}(r_\Lambda)|^2. \tag{7}$$

The reduced electric quadrupole ($E2$) transition strength can be computed using the E2 operator, $\hat{Q}_{2\mu} = \sum_{i\in p} r^2_i Y_{2\mu}(\hat{r}_i)$. Notice that we use the bare charge in evaluating the $B(E2)$ strengths, that is, $+e$ for protons and 0 for neutrons and a Λ particle, since our microscopic calculations are in the full configuration space.

Results and discussions.– Let us now apply the microscopic particle-rotor model to $^{9}_{\Lambda}$Be and discuss its low-lying spectrum. To this end, we first carry out the GCM+PN1DAMP calculation for the nuclear core, ^{8}Be. We generate the mean-field states $|\varphi(\beta)\rangle$ with constrained RMF+BCS calculations with quadrupole deformation. The PC-F1 force [33], together with a density-independent δ pairing force with a smooth cutoff factor [34], is adopted. The pairing strengths are $V_n = -308$ and $V_p = -321$ MeV·fm^3 for neutrons and protons, respectively. More numerical details can be found in Ref. [30]. With the solutions of the GCM calculations, we solve the coupled-channels equations by expanding the radial wave function $\mathscr{R}_{j\ell I_c}(r_\Lambda)$ on the basis of eigenfunctions of a spherical harmonic oscillator with 18 major shells. We take the same value for the parameter α_S in the ΛN interaction as in Ref.[32] and vary

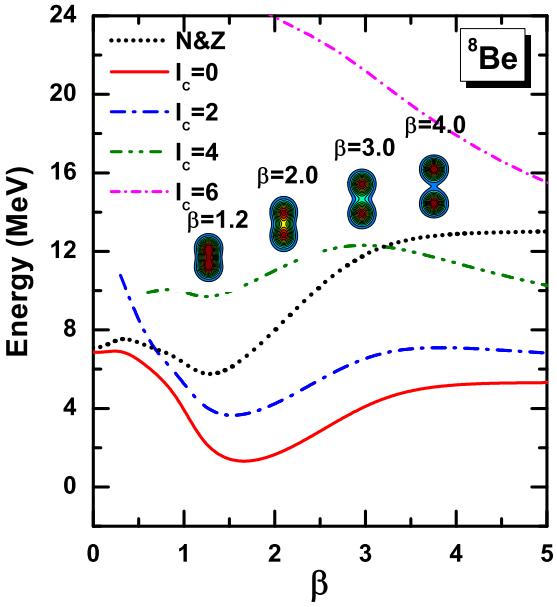

Figure 1: The energy curve for ^{8}Be obtained in the mean-field approximation with the particle number projection (the dotted line) as a function of the intrinsic quadrupole deformation β. The solid, the long dot-dashed, the dot-dot-dashed, and the short dot-dashed lines are projected energy curves for $I_C = 0, 2, 4$, and 6, respectively. The contour plots of the intrinsic densities for $\beta = 1.2, 2.0, 3.0$ and 4.0 are also shown.

the value of α_V so that the experimental Λ binding energy of $^9_\Lambda$Be, $B_\Lambda^{(\mathrm{exp.})}(^9_\Lambda\mathrm{Be})$=6.71±0.04 MeV [35], is reproduced with the microscopic particle-rotor model. The resultant values are $\alpha_S^{N\Lambda} = -4.2377\times10^{-5}\,\mathrm{MeV}^{-2}$ and $\alpha_V^{N\Lambda} = 1.2756\times10^{-5}\,\mathrm{MeV}^{-2}$. The cut-off of the angular momentum for the core states (I_c) is chosen to be 4, which gives well converged results for the low-lying states of $^9_\Lambda$Be. We include only the bound core states, that is, the lowest energy state for each value of I_c, even though all the possible states, including continuum states, should be included in principle.

The dotted line in Fig. 1 shows the energy curve for ^{8}Be obtained in the mean-field approximation with the particle number projection, as a function of the intrinsic quadrupole deformation β. The energy curves with an additional projection onto the angular momentum are also shown in the figure. The density distributions in the mean-field approximation are plotted for β = 1.2, 2.0, 3.0, and 4.0, which exhibit the two-α cluster structure. After restoration of the rotational symmetry, the energy minimum for $I_c = 0$ is found at $\beta = 1.5$, while it is at $\beta = 1.2$ in the mean-field approximation. With the increase of the angular momentum I_c, the energy curve becomes softer and eventually the energy minimum disappears at $I_c = 6$. It implies that the 6^+ state in ^{8}Be is unstable against the 2α dissociation, which is consistent with the experimental observation.

The full results of the GCM+PN1DAMP calculation for ^{8}Be are shown in the column (b) in Fig. 2. For a comparison, the results with a single-configuration with $\beta = 1.2$ and the experimental data [36] are also shown in the columns (a) and (c), respectively. Notice that the former corresponds to the conventional particle-rotor model, in which the nuclear shape, and thus, the deformation parameter is assumed to be identical for each I_c state. Notice that in the full calculation the energy minima appear at different deformations for different values of I_c in Fig. 1. One can see in Fig. 2 that the effect of I_c dependence of the deformation parameter as well as the configuration mixing increases the excitation energies of the 2^+_1 and 4^+_1 states in ^{8}Be, which are in closer agreement with the data [36].

We next discuss the spectrum of $^9_\Lambda$Be. Before going to the full coupled-channels calculations, we first show the results of single-channel calculations in the columns (d), (e), and (f) in Fig. 2, where the Λ particle is in the $s_{1/2}$, $p_{1/2}$, and $p_{3/2}$ orbitals, respectively. For the core nucleus states, we use the results of the GCM+PN1DAMP calculations shown in the column (b) in Fig. 2. For the Λ particle in the $s_{1/2}$ orbit, when it is coupled to the core excitation states of 2^+_1 and 4^+_1, the degenerate $(3/2^+, 5/2^+)$ and $(7/2^+, 9/2^+)$ doublet states in $^9_\Lambda$Be are yielded, respectively. We find that the excitation energies of these two doublet states are slightly larger than those of the corresponding excited states of the core nucleus. This is caused by the fact that the energy gain due to the Λ-N interaction is larger in the ground state as compared to that in the other states. For the Λ particle in the $p_{1/2}$ and $p_{3/2}$ orbitals, one obtains the lowest negative parity $1/2^-$ and $3/2^-$ states in $^9_\Lambda$Be. The $1/2^-$ state is higher than the $3/2^-$ state by 0.03 MeV, which reflects the size of spin-orbit splitting in p_Λ state of $^9_\Lambda$Be. The $1/2^-_1$, $7/2^-_1$, $3/2^-_2$, and $5/2^-_1$ states around 10 MeV in the column (f) in Fig. 2 are resulted from the $2^+ \otimes p_{3/2}$ configuration. The order of these states can be understood in terms of the reorientation effect, that is, the diagonal component for the quardupole term in the coupling potential in the coupled-channels equations. On the other hand, for the $2^+ \otimes p_{1/2}$ configuration, in which the Λ particle in the $p_{1/2}$ orbital coupled to the 2^+ state of the core nucleus, the quadrupole term does not contribute, and the $3/2^-$ and $5/2^-$ states are degenerate in energy in the column (e) in Fig. 2. A more detailed discussion on this characteristic appearance of the multiples will be given in the forthcoming publication [37].

The low-energy spectrum of $^9_\Lambda$Be, obtained by mixing these single-channel configurations with the coupled-channels method, is shown in the column (g), (h), and (i) in Fig. 2. The low-lying states are categorized into three rotational bands, whose structures are confirmed by the calculated $B(E2)$ relations. It is remarkable that the present calculation reconfirms such an interesting prediction of the cluster model that the strong coupling of a hyperon to the collective rotation is realized when the Λ is in the p-orbit [3]. Among these rotational bands, the column (h) corresponds to what they called genuine hypernuclear states [3], which are also referred to as the supersymmetric states having the SU(3) symmetry $(\lambda\mu) = (50)$ of s^4p^5 shell-model configuration [38]. These states do not have corresponding states in the ordinary nucleus, ^{9}Be, because of the Pauli principle of the valence neutron. The calculated spectrum is compared with the available data [1, 39] shown in the column (j) in Fig. 2. One can see that a good agreement with the data is obtained with our calculations. According to our calculations, the measured state with excitation energy of 5.80(13) MeV is actually a mixture of two negative-parity

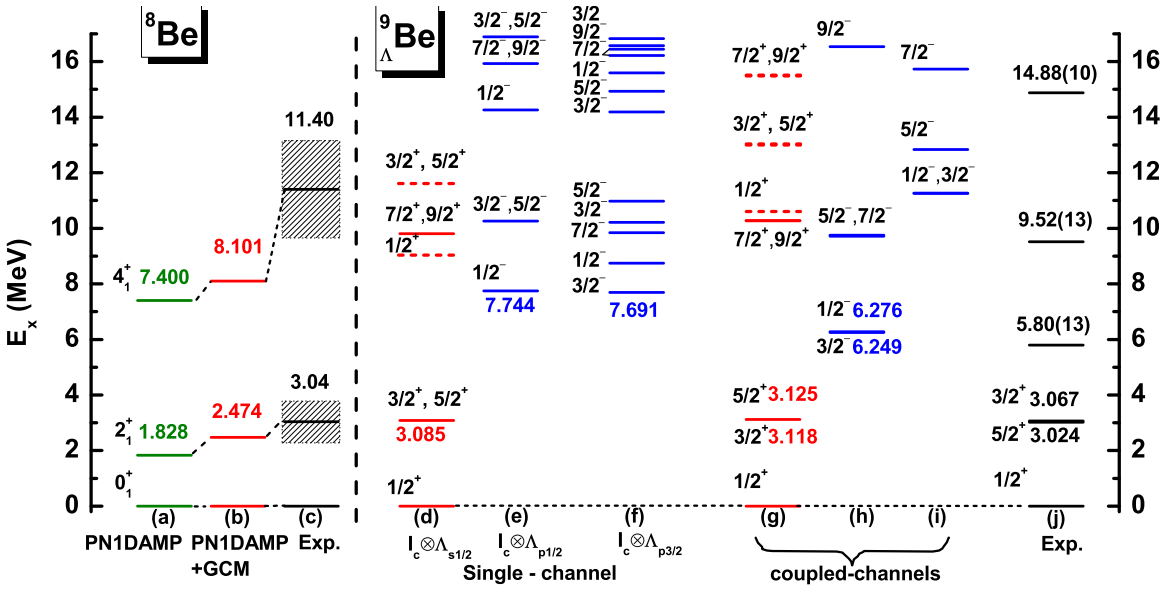

Figure 2: The low-energy excitation spectra of ^{8}Be (the columns (a), (b), and (c)) and $^{9}_{\Lambda}$Be (the columns (d) - (j)). For ^{8}Be, the full GCM+PN1DAMP calculations shown in the column (b) are compared with those without configuration mixing (PN1DAMP: the column (a)) for a single configulation at β=1.2. The experimental data are taken from Ref. [36]. For $^{9}_{\Lambda}$Be, the columns (d), (e), and (f) show the results of the single-channel calculations for the Λ particle in the $s_{1/2}$, $p_{1/2}$, and $p_{3/2}$ channels, respectively. The columns (g), (h), and (i) show the results of the coupled-channels equations, which are compared with the experimental data [1, 39] shown in the column (j).

Table 2: The calculated $E2$ transition strengths (in units of e^2 fm^4) for low-lying states of ^{8}Be and $^{9}_{\Lambda}$Be. c$B(E2)$ is defined by Eq.(8), where L is the total orbital angular momentum.

^{8}Be		$^{9}_{\Lambda}$Be			
$I^\pi_i \to I^\pi_f$	$B(E2)$	$I^\pi_i \to I^\pi_f$	$(L^\pi_i \to L^\pi_f)$	$B(E2)$	cB(E2)
$2^+_1 \to 0^+_1$	24.99	$3/2^+_1 \to 1/2^+_1$	$(2^+ \to 0^+)$	22.55	22.55
		$5/2^+_1 \to 1/2^+_1$	$(2^+ \to 0^+)$	22.57	22.57
$4^+_1 \to 2^+_1$	47.28	$7/2^+_1 \to 3/2^+_1$	$(4^+ \to 2^+)$	37.43	41.58
		$9/2^+_1 \to 5/2^+_1$	$(4^+ \to 2^+)$	41.55	41.55
		$7/2^+_1 \to 5/2^+_1$	$(4^+ \to 2^+)$	4.152	41.52
		$5/2^-_1 \to 1/2^-_1$	$(3^- \to 1^-)$	13.14	16.90
		$7/2^-_1 \to 3/2^-_1$	$(3^- \to 1^-)$	17.15	17.15

states with $J^\pi = 3/2^-$ and $1/2^-$. The state with excitation energy of 9.52(13) MeV, on the other hand, would be a mixture of $J^\pi = 9/2^+, 7/2^+, 7/2^-, 5/2^-$, and $1/2^+$ states, which are close in energy.

Table 1 lists the values of the probability of the dominant components (with $P_{j\ell I_c} \geq 0.10$) for a few low-lying states of $^{9}_{\Lambda}$Be. The unperturbed energies, $E^{(0)}_{\rm 1ch}$, obtained by the single-channel calculations are also shown for each component. One can see that the positive-parity states in the ground state rotational band are almost pure $I^+_c \otimes \Lambda_{s1/2}$ states, while there are appreciable configuration mixings for the negative-parity states as well as the positive-parity states in the excited band. For instance, for the first negative-parity state, $1/2^-_1$, there is a strong mixing between the $0^+ \otimes \Lambda_{p_{1/2}}$ and the $2^+ \otimes \Lambda_{p_{3/2}}$ configurations with almost equal weights. These large mixtures of collective core wave functions manifest the strong coupling mediated by the p-state hyperon. This is caused by the fact that the unperturbed energies, $E^{(0)}_{\rm 1ch}$, are similar to each other for these configurations due to the reorientation effect. It is interesting to notice that the values of $P_{j\ell I_c}$ obtained in the present calculations are similar to those with the cluster model calculations shown in Fig. 2 of Ref. [3]. We also remark that in the second positive parity states (I^+_2) the Λ_d state is admixed appreciably, while in the second negative parity states (I^-_2) the wave functions have the "out-of-phase" nature in comparison with the corresponding first negative parity states (I^-_1).

Table 2 shows the calculated $E2$ transition strengths for low-lying states of ^{8}Be and $^{9}_{\Lambda}$Be. As has been pointed out in Ref. [3], each state in $^{9}_{\Lambda}$Be can be classified in terms of the total orbital angular momentum L, which couples to the spin 1/2 of the Λ particle to form the total angular momentum I. In order to remove the trivial factor due to the angular momentum coupling for spin 1/2 and see more clearly the impurity effect of Λ particle on nuclear collectivity, we follow Ref. [3] and compute the c$B(E2)$ value defined as,

$$cB(E2: L_i \to L_f) \equiv \hat{L_i}^{-2} \hat{I_f}^{-2} \begin{Bmatrix} L_f & I_f & 1/2 \\ I_i & L_i & 2 \end{Bmatrix}^{-2} B(E2: I_i \to I_f), \qquad (8)$$

where $\hat{I} \equiv \sqrt{2I+1}$. Notice that this quantity is more general than the one introduced in Ref. [13], since the weak coupling does not have to be assumed, although both formulas are equivalent for a single-channel configuration of $|\Lambda_{s_{1/2}} \otimes \Phi_{I_c}\rangle$. The impurity effect of Λ particle on ^{8}Be can be discussed by comparing the $B(E2)$ values in ^{8}Be and the c$B(E2)$ values in $^{9}_{\Lambda}$Be in

Table 1: The probability P_{jlI_c} of the dominant components in the wave function for low-lying states of ${}^{9}_{\Lambda}$Be obtained by the microscopic particle-rotor model. Only those components which have P_{jlI_c} larger than 0.1 are shown. E is the energy of each state obtained by solving the coupled-channels equations, while $E^{(0)}_{\rm 1ch}$ is the unperturbed energy obtained with the single-channel calculations. The energies are listed in units of MeV.

I^π	E	$(l\ j)\otimes I_c$	P_{jlI_c}	$E^{(0)}_{\rm 1ch}$	I^π	E	$(l\ j)\otimes I_c$	P_{jlI_c}	$E^{(0)}_{\rm 1ch}$
$1/2^+_1$	0.000	$s_{1/2}\otimes 0^+$	0.928	0.000	$1/2^+_2$	10.603	$s_{1/2}\otimes 0^+$	0.995	9.035
$3/2^+_1$	3.118	$s_{1/2}\otimes 2^+$	0.919	3.085	$3/2^+_2$	13.034	$d_{3/2}\otimes 0^+$	0.841	11.467
							$s_{1/2}\otimes 2^+$	0.131	11.610
$5/2^+_1$	3.125	$s_{1/2}\otimes 2^+$	0.919	3.085	$5/2^+_2$	12.999	$d_{5/2}\otimes 0^+$	0.845	11.450
							$s_{1/2}\otimes 2^+$	0.125	11.610
$7/2^+_1$	10.267	$s_{1/2}\otimes 4^+$	0.894	9.807	$7/2^+_2$	15.510	$d_{3/2}\otimes 2^+$	0.833	13.804
							$d_{5/2}\otimes 2^+$	0.112	14.124
$9/2^+_1$	10.281	$s_{1/2}\otimes 4^+$	0.894	9.807	$9/2^+_2$	15.483	$d_{5/2}\otimes 2^+$	0.943	13.734
$1/2^-_1$	6.276	$p_{1/2}\otimes 0^+$	0.516	7.744	$1/2^-_2$	11.271	$p_{1/2}\otimes 0^+$	0.575	7.744
		$p_{3/2}\otimes 2^+$	0.445	8.741			$p_{3/2}\otimes 2^+$	0.419	8.741
$3/2^-_1$	6.249	$p_{3/2}\otimes 0^+$	0.524	7.691	$3/2^-_2$	11.258	$p_{3/2}\otimes 0^+$	0.568	7.691
		$p_{3/2}\otimes 2^+$	0.220	10.212			$p_{3/2}\otimes 2^+$	0.220	10.212
		$p_{1/2}\otimes 2^+$	0.217	10.259			$p_{1/2}\otimes 2^+$	0.206	10.259
$5/2^-_1$	9.756	$p_{1/2}\otimes 2^+$	0.625	10.259	$5/2^-_2$	12.835	$p_{3/2}\otimes 2^+$	0.769	10.978
		$p_{3/2}\otimes 2^+$	0.186	10.978			$p_{1/2}\otimes 2^+$	0.226	10.259
		$p_{3/2}\otimes 4^+$	0.150	14.935	$7/2^-_2$	15.729	$p_{3/2}\otimes 2^+$	0.603	9.842
$7/2^-_1$	9.717	$p_{3/2}\otimes 2^+$	0.813	9.842			$p_{1/2}\otimes 4^+$	0.216	15.926
		$p_{1/2}\otimes 4^+$	0.100	15.926			$p_{3/2}\otimes 4^+$	0.157	16.215

Table 2. One can see that the $E2$ strengths are slightly decreased due to the shrinkage effect of Λ hyperon.

The degree of reduction in $B(E2)$ with the present model is much smaller than the results of cluster model calculations [3, 40]. Also, the energy of the 2^+ state increases significantly by adding a Λ particle, whereas the experimental data indicate that the energy shift is negligibly small [40] (see Fig. 2). These would be due to the effects of higher members of the core excited states, which are not included in present calculations. However, with the current implementation of GCM, we have a limitation in constructing the wave functions for the non-resonant core states (that is, the second and the third 0^+, 2^+, and 4^+ states), which extend up to large values of deformation parameter β. For this reason, we did not obtain reasonable results for the hypernuclear states above $5/2^+_1$ when we included the higher members of the core states.

Summary.– In summary, we have proposed a novel method for a low-lying spectrum of hypernuclei based on a mean-field type approach. Whereas the pure mean-field approximation does not yield a spectrum due to the broken rotational symmetry, we employed a beyond relativistic mean-field approach by carrying out the angular momentum and the particle number projections as well as the configuration mixing with the generator coordinate method. In this novel method, the beyond mean-field approach is applied to low-lying states of the core nucleus, to which the Λ hyperon couples in the wave function of hypernuclei, and thus we call it the microscopic particle-rotor model. We emphasize that this is the first calculation for a spectrum of hypernuclei based on a density functional approach. By applying the microscopic particle-rotor model to ${}^{9}_{\Lambda}$Be, a reasonable agreement with the experimental data of low-spin spectrum has been achieved without introducing any adjustable parameters, except for the $N\Lambda$ coupling strengths, which were determined to reproduce the Λ binding energy.

In this paper, we have assumed the axial deformation for the core nucleus ^{8}Be. An obvious extension of our method is to take into account the triaxial deformation of the core nucleus. One interesting candidate for this is ${}^{25}_{\Lambda}$Mg, for which the triaxial degree of freedom has been shown to be important in the core nucleus ^{24}Mg[18, 30, 41]. Another point which we would like to make is that our method is not restricted to the rotational motion of a core nucleus, but the vibrational motion can also be treated on the equal footing using the generator coordinate method. It will be interesting to apply systematically the present method to many hypernuclei and to study a transition in low-lying spectrum from a vibrational to a rotational characters. An application of our method to ordinary nuclei with an odd number of nucleons is another interesting problem, although a treatment of the Pauli principle would make it more complicated as compared to hypernuclei studied in this paper.

Acknowledgments

This work was supported in part by the Tohoku University Focused Research Project “Understanding the origins for matters in universe”, JSPS KAKENHI Grant Number 2640263, the National Natural Science Foundation of China under Grant Nos. 11305134, 11105111, and the Fundamental Research Funds for the Central Universities (XDJK2010B007 and XDJK2013C028).

References

[1] O. Hashimoto and H. Tamura, Part. Nucl. Phys. **57** (2006) 564.
[2] H. Tamura, Int. J. Mod. Phys. A **24** (2009) 2101.
[3] T. Motoba, H. Bandō, and K. Ikeda, Prog. Theor. Phys. **70** (1983) 189.
[4] T. Motoba, H. Bandō, K. Ikeda, and T. Yamada, Prog. Theor. Phys. Suppl. **81** (1985) 42.
[5] E. Hiyama, M. Kamimura, K. Miyazaki, and T. Motoba, Phys. Rev. C **59** (1999) 2351.
[6] K. Tanida *et al.*, Phys. Rev. Lett. **86** (2001) 1982.
[7] H. Bando, T. Motoba and J. Žofka, Int. J. Mod. Phys. **A 5** (1990) 4021.
[8] E. Hiyama, Y. Kino, and M. Kamimura, Prog. Part. Nucl. Phys. **51** (2003) 223.
[9] R. H. Dalitz and A. Gal, Ann. Phys. (N.Y.) **116** (1978) 167.
[10] A. Gal, J.M. Soper, and R.H. Dalitz, Ann. Phys. (N.Y.) **63** (1971) 53.
[11] D.J. Millener, Nucl. Phys. **A804** (2008) 84; **A914** (2013) 109.
[12] R. Wirth, D. Gazda, P. Navratil, A. Calci, J. Langhammer, and R. Roth, arXiv:1403.3067 [nucl-th] (2014).
[13] M. Isaka, M. Kimura, A. Doté and A. Ohnishi, Phys. Rev. C **83** (2011) 044323; Phys. Rev. C **83** (2011) 054304.
[14] M. Bender, P.-H. Heenen, and P.-G. Reinhard, Rev. Mod. Phys. **75** (2003) 121.
[15] X. R. Zhou, H.-J. Schulze, H. Sagawa, C. X. Wu, and E.-G. Zhao, Phys. Rev. C **76** (2007) 034312.
[16] M. T. Win and K. Hagino, Phys. Rev. C **78** (2008) 054311.
[17] H.-J. Schulze, M. T. Win, K. Hagino, and H. S. Sagawa, Prog. Theo. Phys. **123** (2010) 569.
[18] Myaing Thi Win, K. Hagino, and T. Koike, Phys. Rev. C **83** (2011) 014301.
[19] B.-N. Lu, E.-G. Zhao, and S.-G. Zhou, Phys. Rev. C **84** (2011) 014328.
[20] A. Li, E. Hiyama, X.-R. Zhou, and H. Sagawa, Phys. Rev. C **87** (2013) 014333.
[21] B.-N. Lu, E. Hiyama, H. Sagawa, and S.-G. Zhou, Phys. Rev. C **89** (2014) 044307.
[22] J. M. Yao, Z. P. Li, K. Hagino, M. Thi Win, Y. Zhang, and J. Meng, Nucl. Phys. **A868-869** (2011) 12.
[23] B. Bally, B. Avez, M. Bender, and P.-H. Heenen, Int. J. Mod. Phys. E **21** (2012) 1250026.
[24] A. Bohr and B.R. Mottelson, *Nuclear Structure Vol. II* (Benjamin, Reading, MA, 1975).
[25] P. Ring and P. Schuck, *The Nuclear Many Body Problem* (Springer-Verlag, New York, 1980).
[26] H. Esbensen, B. A. Brown, and H.Sagawa, Phys. Rev. C **51** (1995) 1274.
[27] F. M. Nunes, I. J. Thompson, and R. C. Johnson, Nucl. Phys. A **596** (1996) 171.
[28] T. Tarutina and M. S. Hussein, Phys. Rev. C **70** (2004) 034603.
[29] Y.Urata, K.Hagino, and H.Sagawa, Phys. Rev. C **83** (2011) 041303(R).
[30] J. M. Yao, J. Meng, P. Ring, and D. Vretenar, Phys. Rev. C **81** (2010) 044311; J. M. Yao, H. Mei, H. Chen, J. Meng, P. Ring, and D. Vretenar, Phys. Rev. C **83** (2011) 014308; J. M. Yao, H. Mei, Z. P. Li, Phys. Lett. B **723** (2013) 459; J. M. Yao, K. Hagino, Z. P. Li, J. Meng, and P. Ring, Phys. Rev. C **89** (2014) 054306.
[31] K. Minomo, T. Sumi, M. Kimura, K. Ogata, Y.R. Shimizu, and M. Yahiro, Phys. Rev. Lett. **108** (2012) 052503.
[32] Y. Tanimura and K. Hagino, Phys. Rev. C **85** (2012) 014306.
[33] T. Burvenich, D. G. Madland, J. A. Maruhn, and P. G. Reinhard, Phys. Rev. C **65** (2002) 044308.
[34] S. J. Krieger, P. Bonche, H. Flocard, P. Quentin, and M. S. Weiss, Nucl. Phys. A **517** (1990) 275.
[35] A. Gal, Advances in Nucl. Phys. **8** (1975) 1.
[36] V. M. Datar, Suresh Kumar, D. R. Chakrabarty, V. Nanal, E. T. Mirgule, A. Mitra, and H. H. Oza, Phys. Rev. Lett. **94** (2005) 122502.
[37] H. Mei, K. Hagino, J.M. Yao, and T. Motoba, to be published.
[38] R.H. Dalitz and A. Gal, Phys. Rev. Lett. **36** (1976) 362.
[39] H. Tamura, S. Ajimura, H. Akikawa *et al.*, Nucl. Phys. A **754** (2005) 58c.
[40] K. Hagino and T. Koike, Phys. Rev. C**84** (2011) 064325.
[41] S.W. Robinson and R.D. Bent, Phys. Rev. **168** (1968) 1266.